





## Article

# Chemical Composition of Hydrophobic Coating Solutions and Its Impact on Carbonate Stones Protection and Preservation

Forough Armal<sup>1</sup>, Luís Dias<sup>1</sup>, José Mirão<sup>1,2</sup> , Vera Pires<sup>1,3</sup> , Fabio Sitzia<sup>1</sup>, Sérgio Martins<sup>1</sup>, Mafalda Costa<sup>1</sup>   
and Pedro Barrulas<sup>1,4,\*</sup> 

- <sup>1</sup> HERCULES Laboratory & IN2PAST, University of Évora, Palácio do Vimioso, Largo Marquês de Marialva 8, 7000-809 Évora, Portugal; forough.arman@gmail.com (F.A.); luisdias@uevora.pt (L.D.); jmirao@uevora.pt (J.M.); vlcp@uevora.pt (V.P.); fsitzia@uevora.pt (F.S.); smam@uevora.pt (S.M.); mcosta@uevora.pt (M.C.)
- <sup>2</sup> Department of Geosciences, School of Science and Technology, University of Évora, Colégio Luís António Verney, R. Romão Ramalho, 59, 7000-671 Évora, Portugal
- <sup>3</sup> Laboratory of Mechanical Tests (LEM), School of Science and Technology, University of Évora, Colégio Luís António Verney, R. Romão Ramalho, 59, 7000-671 Évora, Portugal
- <sup>4</sup> Department of Chemistry and Biochemistry, School of Science and Technology, University of Évora, Colégio Luís António Verney, R. Romão Ramalho, 59, 7000-671 Évora, Portugal
- \* Correspondence: pbarrulas@uevora.pt

**Abstract:** The decay diagnosis and conservation of stone-built heritage is becoming a worldwide concern, especially when stone decay causes chromatic changes in the original stone aesthetics, which directly impacts its sociocultural value. Among all the causes of stone decay, water action is identified as the major cause of stone decay and chromatic changes in stone building materials; hence, protective eco-friendly hydrophobic coatings are the efficient and fundamental options to prevent penetrating water into the stone. This paper aims to contribute to tackling water action on natural building stones by studying three different commercial hydrophobic coatings and finding out the correlation between the effectivity, compatibility, and durability of these coatings and the physical, chemical, and mineralogical features of four distinct types of limestone, one calcitic dolomite, four kinds of marble, and one granitoid. Nine different natural stones have been chosen due to their variations in physical, chemical, and mineralogical natures. A multi-analytical approach was adopted through digital microscopy and colourimetry assays to assess the compatibility of the hydrophobic coatings, accelerating ageing in climatic chambers to assess their durability, optical tensiometer analyses to evaluate the hydrophobic effectiveness, and h-XRF and XRPD for determining the chemical and mineralogical composition of stone samples. The results obtained demonstrate that the coating composed of silane/siloxane with modified fluorinated additives (FAKOLITH FK-3 Plus Nano) is the most effective, compatible, and durable coating among the selected hydrophobic coatings. These results can be considered the pioneering steps for developing eco-friendly and cost-effective coatings.



**Citation:** Armal, F.; Dias, L.; Mirão, J.; Pires, V.; Sitzia, F.; Martins, S.; Costa, M.; Barrulas, P. Chemical Composition of Hydrophobic Coating Solutions and Its Impact on Carbonate Stones Protection and Preservation. *Sustainability* **2023**, *15*, 16135. <https://doi.org/10.3390/su152216135>

Academic Editor: Marco Lezzerini

Received: 11 September 2023

Revised: 15 November 2023

Accepted: 16 November 2023

Published: 20 November 2023

**Keywords:** stone decay; stone heritage protection; eco-friendly hydrophobic coatings; carbonate stone



**Copyright:** © 2023 by the authors. Licensee MDPI, Basel, Switzerland. This article is an open access article distributed under the terms and conditions of the Creative Commons Attribution (CC BY) license (<https://creativecommons.org/licenses/by/4.0/>).

## 1. Introduction

Stone, often regarded as one of the most durable and robust construction materials, can deteriorate due to various factors [1]. The decay of stone is a familiar sight for anyone who has closely examined a historic stone building or monument. While there are a handful of stones that appear to be minimally impacted by centuries of exposure to the elements, the majority are susceptible to gradual degradation. This may not be of great consequence if the stone constitutes an unadorned section of a substantial wall—such as in a castle or cathedral. Nevertheless, even a slight degree of deterioration in a finely carved piece of stone can result in the complete loss of the artist's details. A substantial portion of the world's cultural heritage is built from stone, and it is steadily and inevitably vanishing [2].

The most significant contributors to stone deterioration include air pollution, the presence of soluble salts, biodeterioration, and water action [3–6]. Among these factors, water action stands out as a pivotal factor that triggers other causes of stone decay, prompting some to consider it the primary catalyst for such deterioration [7,8]. Water, being capable of transporting soluble salts and dissolving calcium carbonate, poses a particularly potent threat to carbonate-based stones, rendering them highly susceptible to degradation [9]. Furthermore, the mechanical effects of water action on a stone substrate can compromise the integrity of the stone itself [10]. Porous limestones are especially vulnerable, as water can infiltrate deeply into their pores, posing a threat to the underlying calcium carbonate in deeper layers [11,12]. Consequently, carbonate stones fall into a category that is exceptionally susceptible to the deleterious effects of water, demanding heightened attention in terms of preservation and conservation efforts [13]. The preservation of the world's stone heritage is a global concern, underscoring the importance of categorising and identifying stone decay-related issues [14]. Various efforts have been made to establish universal conservation principles. Noteworthy examples include the 1964 “Venice Charter” and the more recent Burra Charter (ICOMOS 1988), which merits wider recognition. While this publication does not delve into conservation principles extensively, it is crucial to acknowledge that multiple stakeholders influence conservation policy, including the architect, art historian, scientist, archaeologist, conservator, owner, and, ultimately, the broader public. Although a scientist may believe strongly in the validity and significance of their findings, there are other parties whose agreement must be secured before those findings influence conservation policy [2].

Initial assessments and stone type identification are essential prerequisites for conducting a proper diagnosis, a critical step in determining the most suitable conservation treatment [15,16]. Preservation and conservation methods must be executed with the appropriate tools and materials, considering factors such as the degree of stone decay, environmental exposure conditions, and the stone element's intended function. Given the paramount role of water action in stone decay, a fundamental approach in stone preservation and conservation involves addressing water penetration, achieved through the application of superhydrophobic protective substances [17].

Hydrophobicity, first observed on the surfaces of lotus leaves by Neinhuis and Barthlott and subsequently patented as the “Lotus effect” in 1998 [18], is attributed to the hierarchical roughness structure of lotus leaves. This structure creates air pockets within grooves beneath the liquid, reducing the contact area between the liquid and the surface [19]. Micro-scale mounds and nano-scale hair-like structures explain the lotus leaf's hydrophobicity and self-cleaning properties [20], factors that should be considered when developing protective coatings for stone materials. Protective coatings not only reduce the need for extensive repair and maintenance of stone structures but also offer a cost-effective and time-saving long-term approach to preserving their cultural value over time [18].

Historically, techniques for imparting water repellency relied on the application of organic substances, such as resins, acrylate-based compounds, and waxes [1]. However, these compounds have drawbacks, including high viscosity, colour changes, and gloss alterations that result in the formation of thick, coloured coatings [21]. Moreover, formulations based on organic compounds may exhibit insufficient compatibility with ancient stone and, in some cases, pose toxicity concerns upon removal from the substrate [22].

Solvent-based treatments for water repellency were also commonly employed in the past [1]. In this approach, a solution containing a polymer (or its monomers) is applied to the substrate, requiring protection, and the desired film forms as the solvent evaporates [23]. While this process ensures effective penetration of the protective layer into the substrate, even its smallest pores, the use of toxic solvents in protective treatments raises significant environmental and health concerns for operators and anyone coming into contact with treated surfaces [24].

The transition from irreversible and toxic compounds to more environmentally friendly and compatible products has become increasingly crucial in the development of new hy-

drophobic coatings. The search for sustainable solutions in stone preservation has led to the introduction of products that repel water, including siliconates, silicones, and siloxanes [25]. Silane and siloxane coatings have been employed on stones as matrices for nanocomposites, which, owing to the nanometric size of their particles, exhibit enhanced superhydrophobic and photocatalytic properties, facilitating the removal of microorganisms and the cleansing of pollutants [26]. However, the use of nanocomposites in cultural heritage may raise concerns about the release of engineered nanomaterials into the environment, as they may be exposed to rainwash and enter the ecosystem [27].

Another category of crucial water-repellent agents is fluoropolymers, known for their low wettability, making them a logical choice for producing hydrophobic materials due to their low energy surface interaction [28]. Nevertheless, fluorinated chemicals, including perfluoroalkylsilanes and fluoroacrylic polymers, present challenges related to high production costs and adverse environmental impacts. These compounds have been identified as contaminants of high concern due to their persistence, toxicity, potential for bioaccumulation, and widespread distribution within the environment [29].

Recognising the sustainability and environmentally friendly aspects, the shift from solvent-based products with high Volatile Organic Compounds (VOCs) content to low- or zero-VOC water-based systems has been gaining traction in the development of eco-friendly, reversible, and compatible products [26]. Consequently, these coatings have gradually transitioned to formulations that eliminate VOCs, thereby mitigating potential adverse effects on the environment and the health of users [26].

In this research, eco-friendly hydrophobic coatings with different chemical compositions will be discussed further. While protective solutions have frequently been developed to decelerate stone deterioration, robust and effective alternatives to be used for stone conservation purposes are still lacking. This study aims to understand the durability, compatibility, and efficiency to confront external weathering factors of commercial hydrophobic coatings and gain insights into the correspondence of their chemical composition with their potential performance in stone heritage.

## 2. Materials and Methods

The materials used in this research have been categorised into two main groups. The first group consists of the stone samples and mock-ups, which have been selected as case studies. The second group of studied materials is composed of three commercial hydrophobic coatings.

### 2.1. Materials

#### 2.1.1. Stone Specimens

Ten natural stones with high commercial value were selected for studying the effects of hydrophobic coatings on stones. These stones include four distinct types of limestone, one calcitic dolomite, four kinds of marble, and one granitoid, all of which are found in Portuguese territory. The selection was based on their different mineralogical and chemical compositions, as well as various physical features such as texture, colour, porosity, roughness, hardness, thermal conductivity, and water vapour permeability. This diversity of properties allows for comprehensive data and results for comparison.

The granitoid was chosen as a non-carbonate benchmark due to its well-known extreme durability, water resistance, low open porosity, and distinct mineralogical and chemical composition. It was used to validate the acquired data and results from all the carbonate samples [30]. Additionally, since testing the compatibility of the coatings regarding potential colour changes was one of the study's objectives, samples were selected to include a wide range of colours, ranging from dark grey to almost white.

#### 2.1.2. Hydrophobic Coatings

Three commercial hydrophobic coatings have been chosen to be studied and compared. FAKOLITH FK-7 (abbreviated to FK-7) is a brownish VOC-free solution made by modi-

fied silane/siloxane micro-nano dispersion in water with particle size from 7 nanometers. CN2 (whose commercial name cannot be mentioned due to copywrite regulations) is an almost colourless transparent VOC-free solution produced by modified silicon dioxide (SiO<sub>2</sub>) nanoparticles. FAKOLITH FK-3 Plus Nano (abbreviated to FK-3) is a milky solution manufactured by micro-nano emulsion free of perfluorooctanoic acid (PFOA) and perfluorooctanesulfonic acid (PFOS) and is based on nano silanes, siloxanes, and novel modified C6 fluorinated compounds free of VOC.

## 2.2. Methods

### 2.2.1. Sample Preparation

#### Stone Samples

The natural stone specimens were processed and analysed as follows. The stone samples were first powdered using the Planetary Ball Mill PM100 (Retsch, Dusseldorf, Germany). The powdered samples underwent analysis through X-ray powdered diffraction (XRPD) to determine their mineralogical composition. Handheld X-ray fluorescence (h-XRF) analysis was performed on pressed pellets made from powdered samples to identify the major elements present in the stones. Mock-ups of the stone specimens were created using a cutting saw (Struers, Copenhagen, Denmark), resulting in two different dimensions:  $30 \times 30 \times 4 \text{ mm}^3$  for various assessments (roughness, colourimetry, digital microscopy, water vapour permeability, static water contact angle, and ageing simulation) and  $50 \times 50 \times 50 \text{ mm}^3$  for hardness, thermal conductivity, and open porosity evaluations. All mock-ups were thoroughly washed with distilled water and then dried in an oven. For each natural stone specimen, four sets of  $30 \times 30 \times 4 \text{ mm}^3$  mock-ups were produced. The first set served as a controlled standard, while the remaining three sets were coated with the commercial solutions FK-7, CN2, and FK-3, as described in the manuscript.

#### Coatings

The preparation process for each coating followed the application guidelines provided by their respective manufacturing companies. For FK-7 and CN2, these coatings were diluted with distilled water at a ratio of 1:10. The diluted solutions were then sprayed onto the set of stone mock-ups. After application, the coated samples with FK-7 and CN2 were left at room temperature for 24 h to ensure complete drying. For FK-3, the application guide recommended a range of ratios for dilution in distilled water, ranging from 1:6 to 1:14, with a higher concentration leading to better water repellence. To balance water repellence with potential colour changes, the middle ratio of 1:10 was used to prepare the FK-3 coating. The diluted FK-3 solution was sprayed onto the third set of stone mock-ups. Following the application guide, a second layer of FK-3 coating was sprayed on the mock-ups while the previous layer had not completely dried. The dual-coated samples with FK-3 were left at room temperature for 24 h to ensure complete drying.

### 2.2.2. Analytical Methodologies and Techniques

The research employed a range of experimental techniques to achieve its objectives. These techniques served four primary purposes: firstly, to provide a comprehensive characterisation of the stone samples, encompassing their physical, chemical, and mineralogical properties; secondly, to evaluate the compatibility of the coatings with the stone substrate; thirdly, to assess how effectively the coatings protected the stone surfaces from water infiltration; and fourthly, to evaluate the durability of the coatings, especially in response to external environmental factors. These methodological approaches collectively facilitated a thorough investigation of the properties and performance of both the stone samples and the applied coatings.

#### Stone Specimens Characterisation

Surface hardness was accessed for all the selected stone samples since material hardness can enhance the resistance of hydrophobic coatings [31]. The surface hardness testing

was performed using an Equotip 550 (Proceq, Schwerzenbach, Switzerland) portable testing device with an impact device D. For each sample, six individual measurements were taken, and the average value and standard deviation were calculated. All measurements were conducted using the same commercial finishing for all the stone specimens (as sawn). Additionally, surface roughness was measured to determine the correlation between the effectiveness of the applied hydrophobic coatings and the surface roughness of the studied samples. The surface roughness of the specimens was assessed using a SurfTest SJ-210 (Mitutoyo, Kanagawa, Japan) device calibrated to ISO 1997 standards [32]. Among the results provided by this portable, non-destructive device,  $R_a$  ( $\mu\text{m}$ )—representing the roughness average of the absolute values of the profile heights of the peak heights across the evaluation length—was selected as the most appropriate parameter for comparison among all the specimens since it is commonly used for this purpose [33,34]. As in the case of the hardness testing, six individual measurements were performed for each sample's surface, and the average value and standard deviation were calculated.

Thermal conductivity provides valuable insights into the physical and mechanical properties of materials [35]. Therefore, the thermal conductivity values of each stone were compared to gain a general understanding of their characteristics for future applications. Thermal conductivity was measured using an ISOMET 2104 Heat Transfer Analyzer (Isomet, VA, USA). Average values and standard deviations for the thermal conductivity of each sample were obtained by placing the probe in three different locations on its polished surface.

Open porosity, on the other hand, is directly related to water vapour permeability and can influence the compatibility of hydrophobic coatings with stone samples [36]. To investigate the role of open porosity in the studied hydrophobic coatings, an open porosity test for each sample was conducted following the test protocol outlined in European Standard EN 1936 [37]. The experiments were conducted at a room temperature of  $24 \pm 1$  °C, maintaining a relative humidity range of  $50 \pm 5\%$ . Prior to the test, samples were dried for 24 h at  $60 \pm 5$  °C in the oven and then allowed to cool in a desiccator for approximately 8 h at room temperature. Each dried specimen was weighed ( $m_d$ ) before being placed into a vacuum vessel, where the pressure was gradually reduced to reach about  $2.0 \pm 0.7$  kPa ( $=15 \pm 5$  mm Hg). The samples were evacuated, partially submerged, for 2 h to remove trapped air. Demineralised water was then slowly added to the container until all the specimens were submerged. Subsequently, the pressure was returned to atmospheric, and the samples remained submerged in water for an additional 24 h. Each sample was weighed after submersion in both water ( $m_h$ ) and air, and the surface was dried ( $m_s$ ). Open porosity ( $P_0$ ) as a percentage was calculated using Equation (1) [38]:

$$P_0 = \frac{m_s - m_d}{m_s - m_h} \cdot 100 \quad (1)$$

Water vapour permeability tests were conducted to assess the breathability and, consequently, the compatibility of hydrophobic coatings with the studied stone samples. The cup method was employed to measure water vapour transmission, which allowed for the determination of water vapour permeance [39]. According to the technical criteria outlined for Water Vapour Permeability Coefficients ( $W_{VP}$ ), measurements were performed in  $\text{g m}^{-1} \text{s}^{-1} \text{Pa}^{-1}$  using a gas-flow method with a constant pressure differential applied across the specimen. To estimate the water vapour flux,  $G_w$ , the average of the differences between mass per unit time (in g/h) from at least three values obtained during steady-state flow was calculated.  $W_{VP}$  was determined in  $\text{g m}^{-1} \text{s}^{-1} \text{Pa}^{-1}$  using Equation (2):

$$W_{VP} = \frac{G_w \cdot h}{A_s \cdot \Delta P^1 \cdot 36 \times 10^5} \quad (2)$$

where  $G_w$  is water vapour flux;  $h$  is the thickness of specimens;  $A_s$  is the specimens tested area; and  $\Delta P^1$  is vapour pressure inside and outside the container differs. Before conducting

the permeability measurements, the specimens underwent a preparation process. They were initially dried for 24 h at  $60 \pm 5$  °C in an oven and then placed in a desiccator for an additional 24 h. Each dry specimen was individually weighed ( $m_d$ ). Special containers were prepared, filled with cotton and 1 cm of distilled water to create a fully humid environment. Subsequently, each stone specimen was placed on the container's surface, and silicone mastic was used to seal any potential air entry points. Each set comprising the container, water, and stone specimen was weighed in milligrams and then introduced into the FitoClima 600 (Aralab, Rio de Mouro, Portugal) climatic chamber, maintained at a temperature of 20 °C and a relative humidity of 40%. The sets were periodically weighed every 24 h until they exhibited a mass difference of 0.1%, at which point the experiment was concluded.

The elemental composition of the stone samples was determined using h-XRF to explore potential relationships between their composition and the compatibility, effectiveness, and durability of the applied coatings. Measurements were conducted using the Tracer III-SD (Bruker, Billerica, MA, USA) portable spectrometer with a current and voltage of 40 kV and 11  $\mu$ A. The device features a silicon drift X-Flash SDD detector with a Peltier cooling system and a spot size of 3 to 4 mm. The sample surface was brought into contact with the instrument's window, and for each stone, three different spectra were collected, with each spectrum acquired for 60 s. Data were collected using the S1PXRF<sup>®</sup> software (ver. 3.8.30), and the spectra were analysed using the ARTAX<sup>®</sup> software (ver. 7.4.0). The obtained data were normalised using the Rh K $\alpha$  peak.

Given that the hydrophobicity of the stone surface may be related to its mineral composition, XRPD was employed to identify the mineralogical compositions of each stone sample and uncover potential correlations between mineralogical composition and the effectiveness of the applied coatings [40]. XRPD measurements were carried out using a D8 Discover (Bruker, Billerica, MA, USA) diffractometer, utilising Cu-K $\alpha$  radiation ( $\lambda = 0.15406$  nm), operating at 40 kV and 40 mA. Powder diffraction data were collected in steps of 0.05° with a measuring duration of 1 s in the range of 5–75° (2 $\theta$ ). The obtained XRPD patterns were identified using the PDF-2 X-ray patterns database of the International Centre for Diffraction Data and the DIFFRAC.SUITE EVA software (ver. 5.1.0.5) was employed for analysis.

#### Coating Compatibility Assays

Chromatic changes become particularly significant when dealing with heritage stones [41]. Alterations in colour can stem from staining caused by foreign substances such as, for example, dust particles transported in water, salts dissolved in water, lichens, fungus, or other bio colonisation agents. Evaluating stone colour stability, as well as the natural colour of the stones, is essential for assessing the compatibility of protective coatings that may be applied to them. To minimise errors arising from surface heterogeneity, the central area of each mock-up was examined at each stage. The colour was measured by determining the CIELAB parameters using a Check II Plus (Datacolor, Risch-Rotkreuz, Switzerland) with the USAV aperture. After three measurements, average coordinates and standard deviations were calculated. Colourimetry measurements allowed for the assessment of the colour difference on the surface of each mock-up before and after treatment, as well as after the ageing process. Colour differences can be quantified as a single numerical value,  $\Delta E^*$  (Equation (3)), which indicates the magnitude of the colour difference without specifying the nature of the difference [25,42]:

$$\Delta E^* = [(L_t^* - L_0^*)^2 + (a_t^* - a_0^*)^2 + (b_t^* - L_0^*)^2]^{1/2} \quad (3)$$

where “0” stands for the reference stone specimen's initial colour, and “t” stands for the altered stone specimens' colour following any hydrophobic coatings treatment or accelerated ageing test [43].

According to the CIELAB system, when  $\Delta E^*$  (total colour difference) equals 1, the colour change is barely discernible to the naked eye, becoming noticeable at around  $\Delta E^*$

≈ 2–3 [25]. However, when dealing with the conservation and restoration of historic structures,  $\Delta E^* < 5$  is often regarded as the acceptable threshold for colour change [25].

A HRX-01 (Hirox, Tokyo, Japan) digital microscope was also used to document the stone specimens before and after their treatment and after the ageing procedure.

#### Hydrophobic Effectiveness

Static water contact angle measurements are essential to assess surface hydrophobicity [44,45]. Contact angle measurements can be an extremely valuable technique for evaluating the effectiveness of hydrophobic treatments on stones [46–48]. In this study, static water contact angle measurements were particularly useful for comparing the effects of hydrophobic coatings on different selected stone samples and their changes after ageing. The measurements were conducted using a Ramé-Hart Model 210 Goniometer/Tensiometer (Ramé-Hart, Succasunna, NJ, USA). In this procedure, a pipette was filled with deionised water, and a droplet was placed on a sample holder with the test surface in a horizontal position. To obtain a reliable average assessment, the contact angle of the droplet deposited on a stone surface was measured between 3 to 10 s for each sample. Twelve drops were placed on each sample surface, and for each drop, four measurements were recorded [49]. The obtained values were averaged, and the standard deviation was calculated. Images and data were acquired and processed using the DROPimage software (ver. 3.21.11.0).

#### Durability Assessment

Several studies have focused on assessing the durability of hydrophobic treatments on stone when exposed to simulated weather conditions in laboratory-controlled ageing experiments [50,51]. Therefore, this study aimed to evaluate the durability of the applied coatings on stone samples by comparing their colour, water vapour permeability, and contact angle before and after undergoing an ageing simulation. The samples were subjected to weathering cycles using the QUV-Accelerated Weathering Tester (Q-Lab, College Park, MD, USA) following the ASTM G154-C7 standard method [52]. This method involves 15 min of water spray and 3 h 45 min of condensation at 50 °C, along with 8 h of UVA radiation at 340 nm and 60 °C (with an irradiance of 1.55 W/m<sup>2</sup>). Each cycle lasted 12 h, and a total of 30 cycles were applied [53]. The colour, contact angle, and water vapour permeability of the samples were evaluated both before ageing (at time 0) and after ageing.

### 3. Results and Discussion

The present study investigated the compatibility, effectiveness, and durability of several commercial coatings. The work combined a multi-analytical approach to reach comprehensive results. These findings have important implications for the potential preservation of natural stone since they will pave the way for the development of new effective solutions.

#### 3.1. Characterisation of Stone Specimens

The analysis began by characterising the physical properties of the stone specimens, including hardness, roughness, thermal conductivity, open porosity, and water vapour permeability. Results of the physical properties of the studied stone samples are presented in Table 1.

The results of the surface hardness test showed that the surface hardness of all the studied samples ranged from  $459.2 \pm 54.0$  to  $862.0 \pm 25.9$  HLD (Table 1). The highest value of surface hardness belongs to G1. Among the carbonate stone samples, M1 and L2 have the lowest rate for surface hardness, respectively (Table 1). According to Mohs's hardness scale, which determines minerals' resistance to abrasion or scratching, minerals are ranked with the numerical value related to their hardness from 0 to 10 (qualitative ordinal scale) [54]. Hence, different materials can have a numerical range of values to compare their hardness [55]. When it comes to stone materials, the hardness of the minerals present determines the hardness of stone [56]. Therefore, the granitoid, composed primarily

of quartz, K-feldspar, and plagioclase (between 6.5 and 7 on the Mohs's hardness scale) and other silicate-based minerals, has a rather high degree of hardness, around 7. On the other hand, marble, and limestone, where calcite (3 on the Mohs's hardness scale) is a major component, have hardness values much lower than granitoid. Besides being a benchmark in this study, this gives the granitoid a higher hydrophobic potential [57].

**Table 1.** Physical characterisation measurements (Hardness, Roughness, Thermal Conductivity, Open Porosity, and water vapour permeability) of stone specimens.

Ref N.	Typology	Hardness (HLD)		Roughness Ra ( $\mu\text{m}$ )		Thermal Conductivity $\lambda$ ( $\text{Wm}^{-1}\text{K}^{-1}$ )		Open Porosity (%)		Water Vapour Permeability $W_{VP}$ ( $\text{g m}^{-1} \text{s}^{-1} \text{Pa}^{-1}$ )
		Mean	Stdev	Mean	Stdev	Mean	Stdev	Mean	Stdev	
L1	Limestone	535.5	8.6	5.9	1.6	2.1	0.0	13.3	0.2	$6.0 \times 10^{-12}$
L2	Limestone	478.8	21.0	3.5	1.2	2.0	0.0	11.3	0.3	$6.3 \times 10^{-12}$
L3	Limestone	696.2	6.6	2.5	0.8	2.5	0.0	8.5	0.1	$2.3 \times 10^{-12}$
L4	Limestone	570.7	36.8	3.4	1.0	2.4	0.0	0.4	0.0	$8.9 \times 10^{-12}$
L5	Calcitic dolomite	665.3	15.2	2.7	0.3	2.4	0.0	1.2	0.1	$7.7 \times 10^{-12}$
M1	Marble	459.2	54.0	3.3	0.6	2.5	0.0	0.2	0.0	$2.2 \times 10^{-12}$
M2	Marble	533.7	47.2	2.3	0.2	2.3	0.0	0.5	0.0	$4.7 \times 10^{-12}$
M3	Marble	573.7	33.1	4.3	0.1	2.5	0.0	0.2	0.0	$5.1 \times 10^{-12}$
M4	Marble	554.8	30.1	4.9	0.9	2.2.6	0.0	0.3	0.0	$3.8 \times 10^{-12}$
G1	Granitoid	862.0	25.9	4.0	1.1	2.5	0.0	0.7	0.1	$5.5 \times 10^{-12}$

Based on the surface roughness test results, the range of surface roughness of studied samples is from  $2.3 \pm 0.2$  to  $5.9 \pm 1.6 \mu\text{m}$ . This range for carbonate sedimentary rocks is from  $2.5 \pm 0.8$  to  $5.9 \pm 1.6 \mu\text{m}$ , and for marbles is between  $2.3 \pm 0.2$  and  $4.9 \pm 0.9 \mu\text{m}$  (Table 1). Therefore, the roughest surface among carbonate sedimentary rocks belongs to sample L1, and among marbles belongs to sample M4. According to Wenzel's theory [58], enhancement in surface roughness of a surface will increment its wettability. Additionally, surface roughness can cause both hydrophobic surfaces to become increasingly more hydrophobic and hydrophilic surfaces increasingly more hydrophilic [59]. Cassie and Baxter, on the other hand, postulated that surface roughness can enhance hydrophobicity [59]. Therefore, the hydrophobicity of the surfaces directly relates to their roughness. As such, the results suggest that samples L1 and M4 have lower hydrophobicity potential than the remaining carbonate sedimentary rocks and marble specimens.

Table 1 also displays the thermal characteristics of studied samples of dry stones at ambient pressure (1 atm) and temperature (25 °C). Carbonate sedimentary rocks are found to have thermal conductivities between 2.0 and  $2.5 \text{ Wm}^{-1}\text{K}^{-1}$ , while that of the marble samples range from 2.3 to  $2.6 \text{ Wm}^{-1}\text{K}^{-1}$ . The thermal conductivity of the granitoid sample is  $2.5 \text{ Wm}^{-1}\text{K}^{-1}$  (Table 1). Amaral and co-authors assessed the quality of several Portuguese building stones considering several parameters, including thermal conductivity [60]. According to this study, stones with thermal conductivity values between 0.3 and  $4.0 \text{ Wm}^{-1}\text{K}^{-1}$  have medium quality for civil construction [60]. Therefore, based on this classification, all the studied samples in this research are similar, presenting medium thermal conductivity and average stone quality for building purposes.

According to Table 1, the range of open porosity of studied samples is from 0.2 to 13.30%. This range for carbonate sedimentary rocks is 0.4 to 13.3%, while for marbles, the open porosity values range between 0.2 and 0.5%. Therefore, the variability of open porosity is highly noticeable among carbonate sedimentary rocks but constant in marbles. The open porosity of the granitoid (G1) is closer to that of marbles: 0.7% (Table 1). The elevated open porosity percentage observed in carbonate sedimentary rock samples, particularly in L1, L2, and L3, aligns with commonly reported characteristics of these stone specimens. This consistency arises from the inherent porosity of limestones, which tends to be higher



compared to marbles and granitoids. This difference can be attributed to distinct diagenetic processes influencing the formation of these rock types [12].

Differences in permeability were expected in accordance with the typical distinction for porous networks among limestones, dolomites, marbles, and granitoids [61]. Hence, the carbonate sedimentary rocks analysed have a higher amount of water vapour permeability when compared to the other stone specimens analysed, especially samples L1, L2, L4, and L5 (Table 1).

Chemical and mineralogical characterisation of the stone specimens was also carried out by h-XRF and XRPD. The results of XRPD, which can be found in Table 2, revealed compositional differences within the carbonate sedimentary rocks and marble stone specimens. While most of the selected sedimentary rocks are limestones, composed primarily of calcite with small amounts of quartz, specimen L5 is a calcitic dolomite composed of both calcite and dolomite, with the latter being more abundant. As expected, calcite was also found to be the main mineral phase present in all marble stone specimens, accompanied by quartz in variable amounts. Illite/muscovite was also found in significant amounts in most samples (except M4), and plagioclase is present in both M2 and M4. It is important to highlight specimen M1 due to the abundance of illite/muscovite and the detection of minor or trace amounts of amphibole in its composition. The granitoid specimen is composed of quartz, plagioclase, alkali feldspar, biotite, and chlorite.

**Table 2.** Mineral phases identified by XRPD in the stone specimens (Abbreviations: +++ = very abundant, ++ = abundant, + = present, tr = trace).

Ref N.	Typology	Mineral Phases								
		Calcite	Dolomite	Quartz	Amphibole	Plagioclase	K-Feldspar	Illite/Muscovite	Biotite	Chlorite
L1	Limestone	+++	-	tr	-	-	-	-	-	-
L2	Limestone	+++	-	tr	-	-	-	-	-	-
L3	Limestone	+++	-	+/tr	-	-	-	-	-	-
L4	Limestone	+++	-	tr	-	-	-	-	-	-
L5	Calcitic dolomite	++	+++	-	-	-	-	-	-	-
M1	Marble	+++	-	+	+/tr	-	-	++	-	-
M2	Marble	+++	-	+/tr	-	+/tr	-	++	-	-
M3	Marble	+++	-	tr	-	-	+/tr	++	-	-
M4	Marble	+++	-	tr	-	+/tr	-	-	-	-
G1	Granitoid	-	-	++	-	+++	+	-	+/tr	++

The h-XRF results are in accordance with the XRPD data, with low contents of silicon being detected in the carbonate stone specimens, in contrast to the granitoid non-carbonate benchmark analysed (Figure 1a). The lower Ca content of stone specimen L5 can be explained by the abundance of dolomite ( $\text{CaMg}(\text{CO}_3)_2$ ) in its mineralogical composition. Elements with low atomic numbers are generally difficult to detect using h-XRF instruments due to the strong absorption of low-energy X-rays by air and by the Be window of the detector [55]. Elements with  $Z < 13$  have previously been found to be poorly identifiable using the Bruker Tracer III-SD instrument [62], which can explain the absence of Mg in the spectra of specimen L5. As expected, the granitoid specimen also contains much higher amounts of Fe (Figure 1b) and K, which can be linked to its mineralogical composition, namely the presence of biotite and alkali feldspars. All carbonate stones analysed have similar composition; however, as seen in Figure 1c,d, there are some small differences that must be highlighted. Marble specimen M1 has significant Mn contents (Figure 1c), which is likely associated with the presence of amphibole in its composition, as identified by XRPD (Table 2). Manganese is a common impurity in the tremolite-actinolite series, amphibole phases that have previously been identified in similar marble specimens [63]. Barium was also detected in specimens L1, M1, and M4 (Figure 1d). While barium is likely present in the form of barite in trace amounts in specimen M1 [63], its incorporation into the structure of calcite in all aforementioned specimens cannot be disregarded.  $\text{Ba}^{2+}$  is known to be highly incompatible with calcite, preferring to incorporate the larger structure

of the polymorph aragonite [64]. Nevertheless, calcite can still contain small amounts of Ba [65].

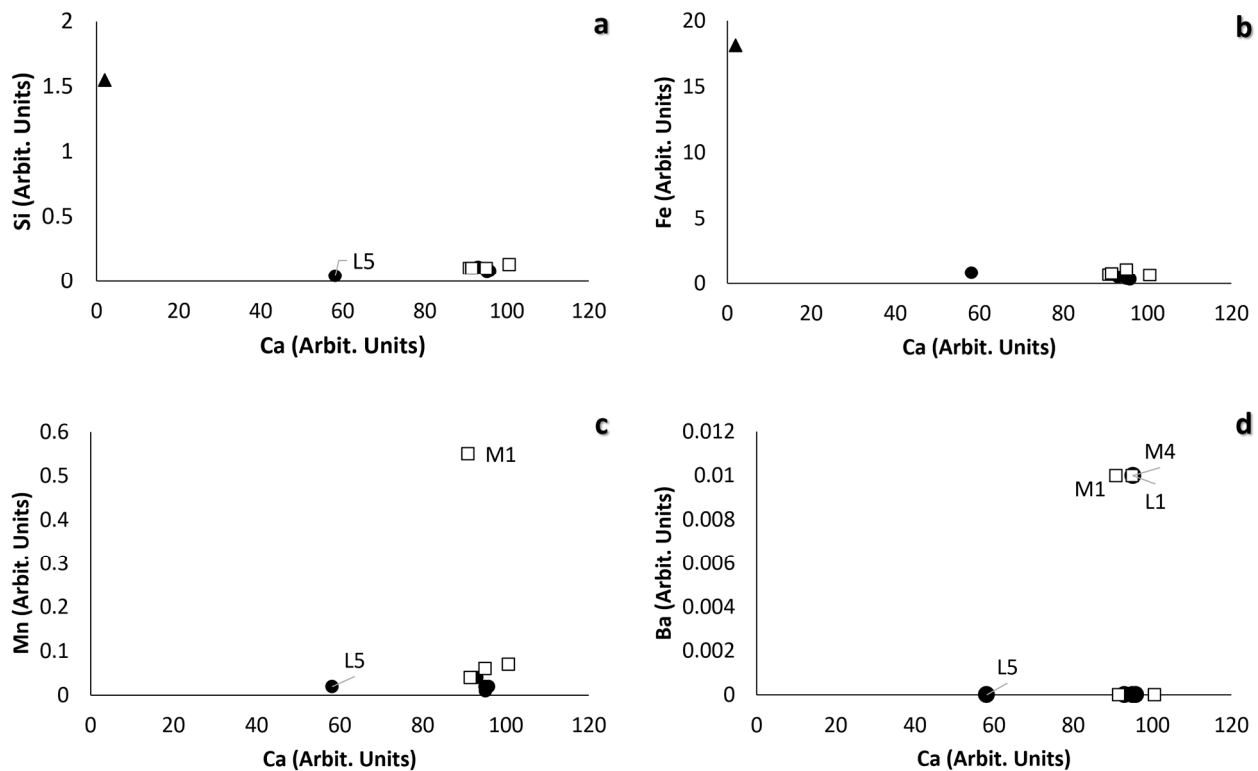


**Figure 1.** Elemental bi-plots of Si-Ca (a), Fe-Ca (b), Mn-Ca (c) and Ba-Ca (d) revealing compositional differences between the different stone specimens analysed by h-XRF.

### 3.2. Chromatic Change Evaluation

#### 3.2.1. Compatibility of Hydrophobic Changes

Colour changes are typically the initial alterations that become noticeable to the naked eye before any other analyses are conducted. However, when developing new solutions for protecting stone materials, visible colour variation is generally considered an undesirable characteristic as it can impact both the aesthetics and the commercial value of the material.

The colour difference for each sample was calculated after applying the coating and after subjecting it to the accelerated ageing chamber. Coatings that resulted in a  $\Delta E^* \geq 5$  were considered incompatible with the stone substrate. In the graphical representation shown in Figure 2, visible colour changes indicating incompatibility with the stone substrate are marked in red.

According to Figure 2, the difference in colour change in FK-7 before and after treatment is less than 5, except in samples L2, M4, and G1. The colour changes for CN2 when applied on marbles and the granitoid specimen are also within the acceptance threshold considered in this study ( $\Delta E^* < 5$ ). However, when applied to the carbonate sedimentary rocks samples, coating CN2 induced severe colour changes except in sample L3. Coating FK-3, on the other hand, always imparted colour changes within the acceptable zone regardless of the stone specimen to which it was applied. However, it is important to note that the colour changes of FK-3 coated L1 and L2 are close to the incompatible value considered ( $\Delta E^* \geq 5$ ).

These results demonstrate that the chromatic changes observable in the stone samples after treatment could be directly related to the chemical composition of each coating. Notably, FK-7, formulated with a silane/siloxane micro-nano composition, induced only slight colour changes, consistently maintaining relative compatibility ( $\Delta E^* < 5$ ) with most stone specimens. In contrast, CN2 coatings, based on modified silicon dioxide nanoparticles,

resulted in more noticeable colour changes, especially in carbonate sedimentary rock samples. FK-3, which incorporated nano-silane, siloxane, and modified fluorinated compounds, generally maintained compatible colour changes with the stone substrate. However, L1 and L2 were exceptions, approaching the incompatible threshold. These results highlight the differential impact of coating chemical composition on visible colour alterations of stone heritage architectural elements.

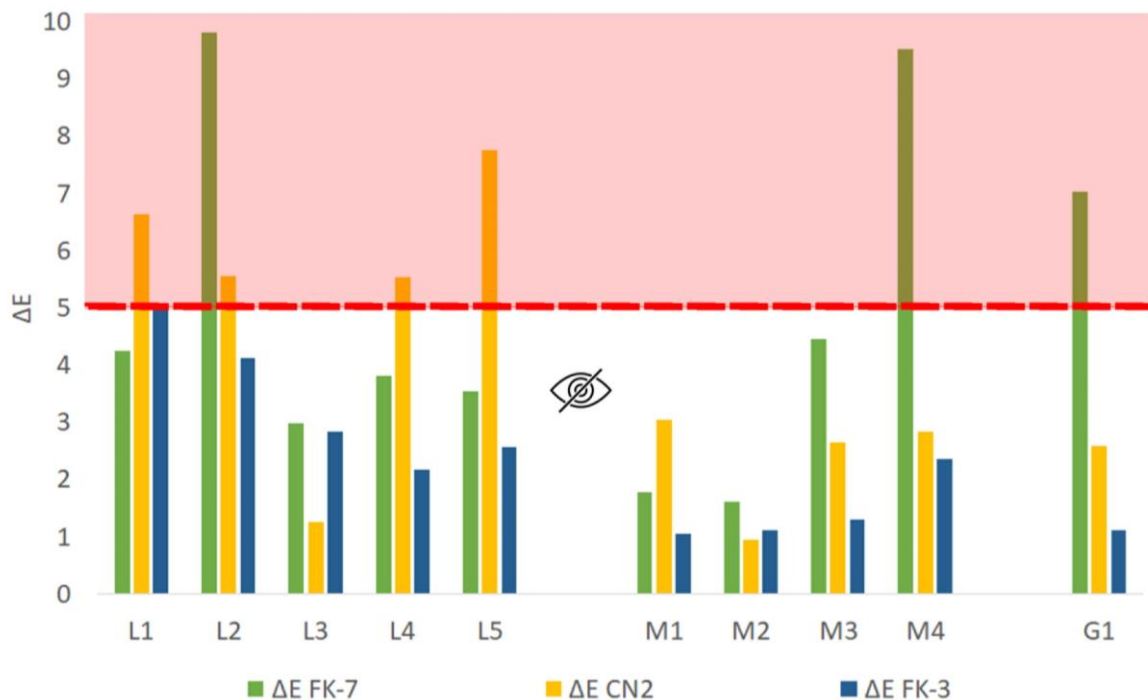


**Figure 2.** Graphic representation of  $\Delta E^*$  for FK-7, CN2, and FK-3 applied on studied stone samples before and after treatment.

### 3.2.2. Durability of Hydrophobic Coatings

When creating new treatments for stone materials, it is essential to ensure that ageing or exposure to different atmospheric conditions does not induce visible colour change. Therefore, in this study, both the compatibility and the durability of the hydrophobic coatings applied were assessed. For the latter, the colour difference from aged mock-ups to non-aged ones was calculated for each specimen. As in the case of the compatibility assessments,  $\Delta E^* < 5$  was the acceptance threshold considered. Figure 3 shows the assessment of the colour changes of the coated stone mock-ups before and after ageing.

In FK-7, the colour change after the ageing process is less than 5 in all the samples. Hence, FK-7 shows acceptable behaviour in the simulated weathering conditions. On the other hand, the colour of samples L2 and G1 coated with CN2 changed beyond  $\Delta E^* < 5$  after the ageing process. However, with this hydrophobic coating, the colour change of the marble samples is not perceptible by the naked eye. Additionally, all the samples coated with FK-3 except the granitoid were found to have acceptable colour changes after the ageing process.

Complementary Figures 3 and 4 present the colour difference between aged mock-up samples and their original states, with the aim of assessing the extent to which the ageing process can alter the initial colouration of the coated specimens. This analysis also serves as an indicator of the durability of the applied coatings and their resistance to colour changes over time.

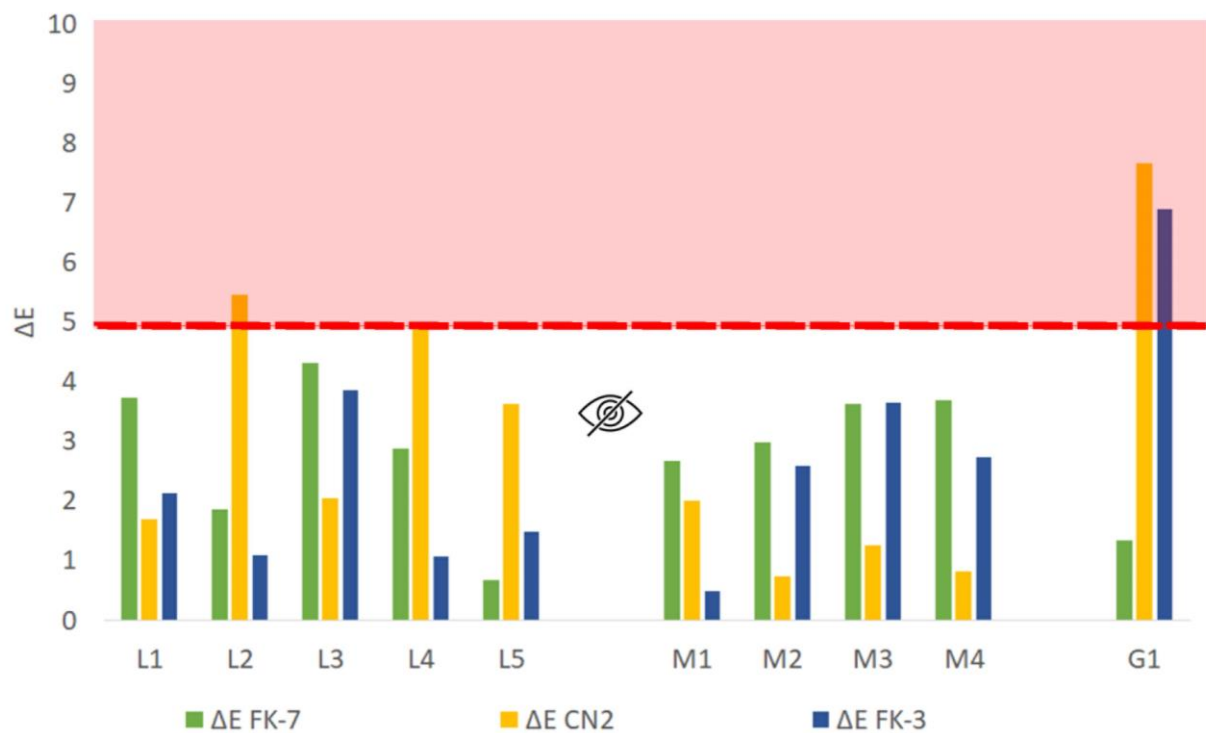


**Figure 3.** Graphic representation of  $\Delta E^*$  for FK-7, CN2, and FK-3 applied on studied stone samples.  $\Delta E^*$  was calculated based on the different colour values of the samples before and after ageing.

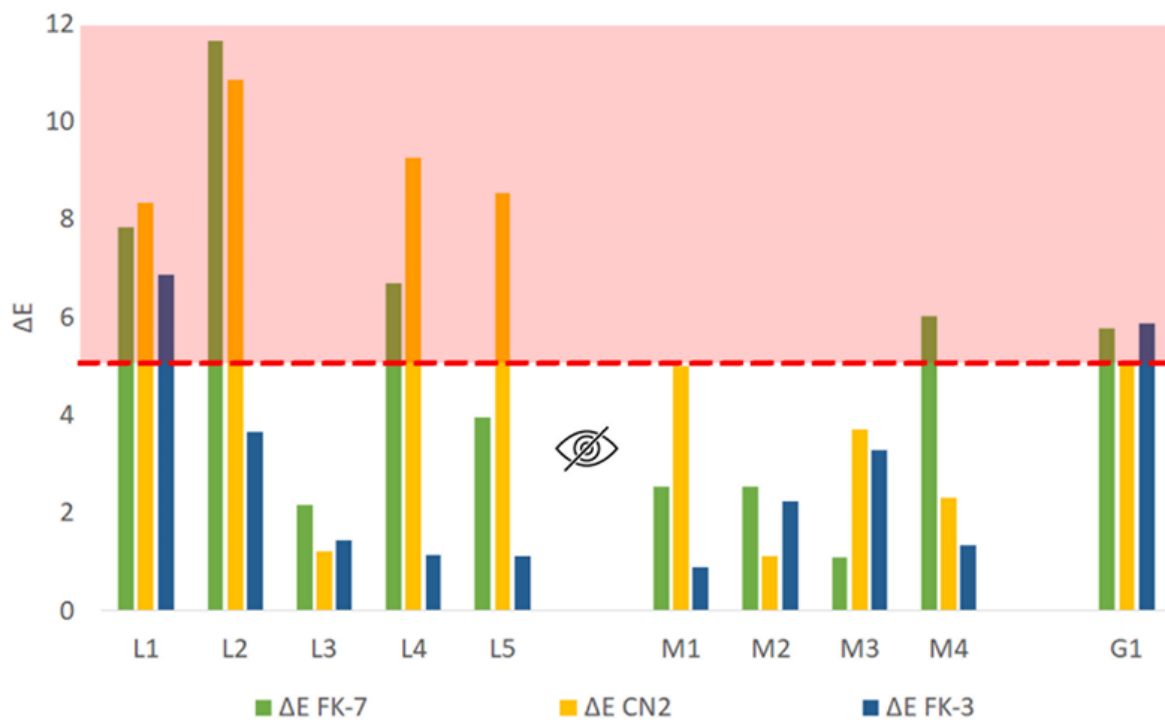


**Figure 4.** Graphic representation of  $\Delta E^*$  for FK-7, CN2, and FK-3 applied on studied stone samples.  $\Delta E^*$  was calculated based on the difference colour values of the original samples and coated ones after ageing.

Figure 4 reveals that FK-7 and CN2 exhibit unacceptable colour changes when applied to several of the stone specimens. Notably, the changes are more tolerable in the context of marble samples (M1, M2, and M3) compared to carbonate sedimentary rocks and the grani-

toid samples. Conversely, specimens coated with FK-3 demonstrate an acceptable degree of colour retention after ageing compared to their original states, except for unacceptable colour changes observed in L1 and G1.

By comparing the results displayed in Figures 2–4, it becomes clear that hydrophobic coating FK-3 displays a higher degree of compatibility and durability. However, it is important to note that the durability of this coating for sample G1, the non-carbonate benchmark, is challenging. Ensuring the long-term durability of hydrophobic coatings is crucial, as they should withstand environmental conditions without significant colour changes. The analysis of coating durability (Figures 3 and 4) revealed that FK-7 exhibited limited durability for aged carbonate sedimentary rock samples but remained more acceptable for aged marble samples. FK-3 displayed a higher degree of compatibility and durability, apart from sample G1 and L1. CN2 coatings exhibited variable durability but generally performed acceptably, especially in marbles.

### 3.3. Hydrophobic Properties

#### 3.3.1. Hydrophobic Effectiveness

An effective hydrophobic coating exhibits a water contact angle greater than 90 degrees [44,45], while superhydrophobic surfaces can reach 150 degrees or more [66]. Therefore, a stone surface is considered hydrophobic when a water droplet forms an angle of 90 degrees or more (green area in Figure 5). The graphic representation of the contact angle results of coated mock-ups with different coatings and untreated samples (standards) before the ageing process is shown in Figure 5.

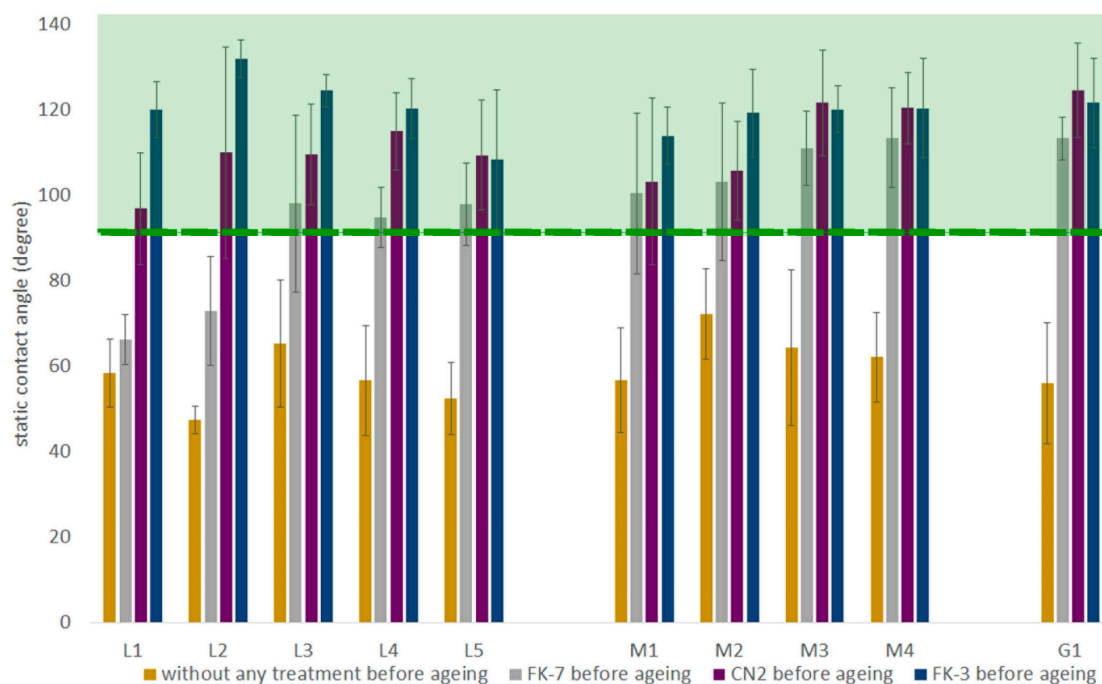


**Figure 5.** Graphic representation of the hydrophobic effectiveness of the coatings studied, based on the static water contact angles of the non-coated and coated mock-ups prior to the ageing test.

As seen in Figure 5, all stone samples coated with FK-3 prior to the ageing process display contact angles higher than 90°, and, as such, have effective hydrophobicity. CN2 also made all stone samples effectively hydrophobic. However, given the high standard deviation in the measurements conducted on samples L1, L2, and M1, it is possible that this coating may not always fulfil the required expectations regarding hydrophobicity. The results also showed that among all the applied coatings, FK-7 has the least hydrophobic effectiveness regardless of the stone surface on which it was applied. Stone specimens L1 and L2 did not become hydrophobic with coating FK-7. All coatings appear to have significant hydrophobic effectiveness when applied to the non-carbonate benchmark G1.

The enhancement values (%) of the contact angles of each sample after applying the different coatings are presented in Figure 5. This percentage has been calculated based on the increased contact angle value after applying coatings compared to untreated mock-ups (standards).

As expected, given the results displayed in Figure 5, FK-7 has the least improvements in hydrophobicity on the surfaces of stone samples when compared to other coatings (Figure 6). The difference enhancement in hydrophobicity caused by the three coatings studied is more noticeable among the carbonate sedimentary rock specimens. In general, mock-ups where the FK-3 coating was applied have the largest enhancement values. Although FK-7 and FK-3 both have the silane-siloxane base composition, the noticeable difference in their compatibility with stone samples could be related to modified fluorinated compounds (C6 chemistry) additives in FK-3. This chemical composition, due to its ultralow surface energy, is known to achieve a well-performed coating functionality [67], which may explain the observable increased effectiveness of FK-3. Therefore, results demonstrated that FK-3 consistently rendered stone surfaces effectively hydrophobic, irrespective of stone type. CN2 coatings also achieved hydrophobicity, but in some cases, particularly with carbonate sedimentary rock samples, displayed variations that might not always meet the required criteria. FK-7, despite its silane/siloxane chemistry like FK-3, exhibited the lowest hydrophobic effectiveness across the board, especially with carbonate sedimentary rock samples.

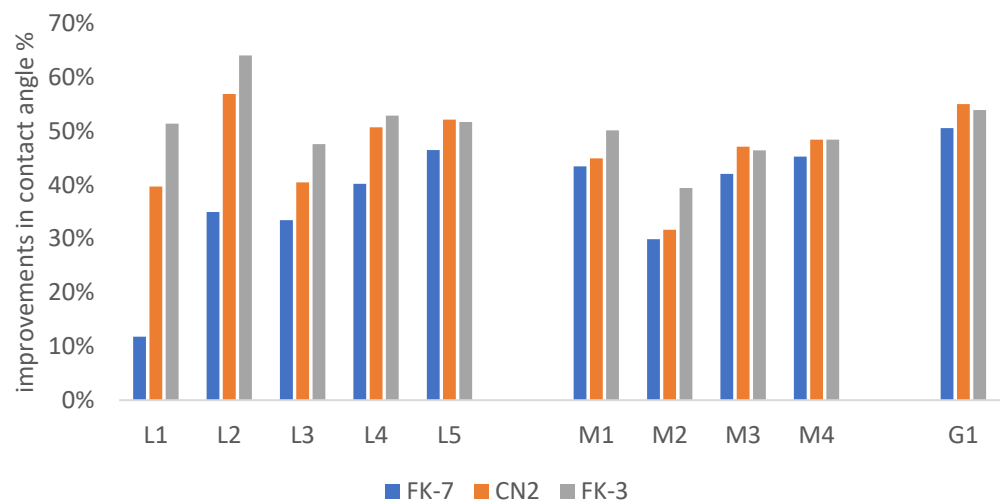


**Figure 6.** Enhancement (%) in hydrophobicity of studied stone samples for each applied coating.

Coating the surface of stones with nanoparticles has been used to make them hydrophobic and, therefore, cause them to strongly repel water [18]. This effect is particularly noticeable in high-porosity stone samples when compared to low-porosity ones [18]. The augmentation of hydrophobicity in FK-3, characterised by micro-nano particles, exhibits varying outcomes in distinct lithotypes distinguished by differing porosity levels. As illustrated in Figure 6, the hydrophobicity effectiveness of FK-3 on limestones and dolomites, with a particular emphasis on samples L1, L2, L3, and L5 characterised by higher porosity levels relative to other samples (as detailed in Table 1), falls within a range of 40% to 57%. This range is marginally higher in comparison to marbles with lower porosity levels (Table 1), where the hydrophobicity effectiveness ranges from 32% to 48%. Therefore, while it was not possible to find a strong relationship between the physical and chemical properties of the selected stone specimens and the effectiveness of the hydrophobic coatings, this comparison may indicate a potential correlation between the hydrophobic effectiveness of the FK-3 coating and the porosity of stone lithotypes included in this study.

### 3.3.2. Hydrophobics Durability

The durability of hydrophobic coatings can be affected by natural or artificial weathering [50]. Accelerated ageing with simulation of weathering conditions can, therefore, be used to assess the durability of coatings [68].

The durability of the hydrophobic effectiveness of the three coatings was assessed by comparing the static water contact angles of the coated mock-ups prior to and after being subjected to the ageing process. The graphic representation of the results obtained is depicted in Figure 7, where the green area represents the effective hydrophobic region of the studied samples.

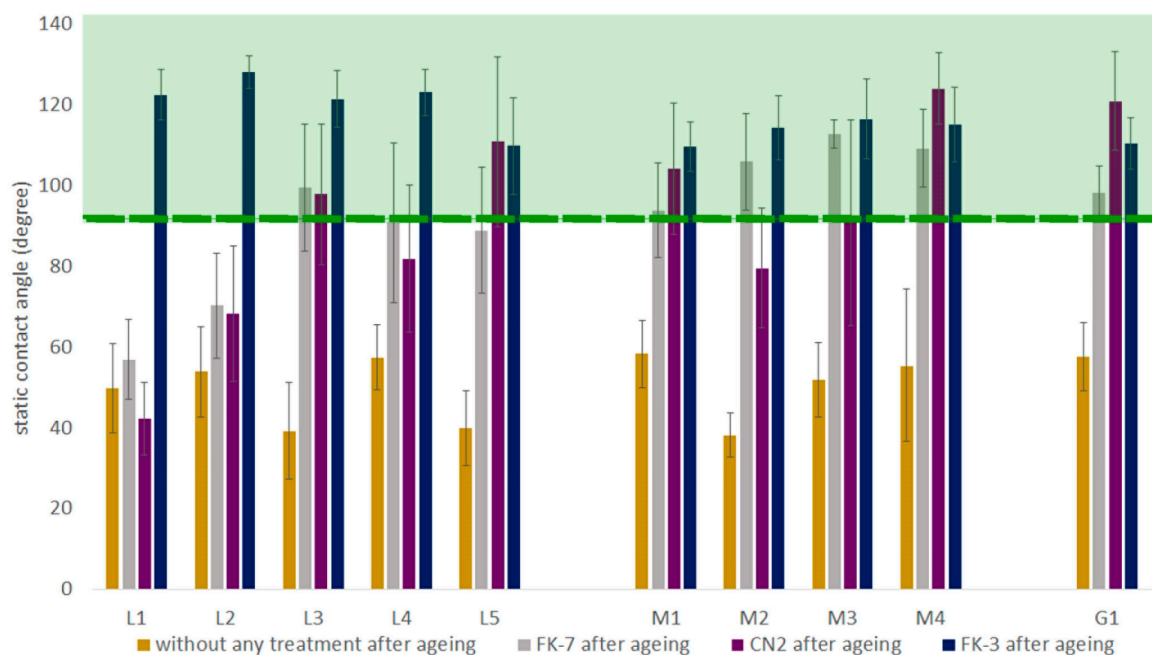


**Figure 7.** Graphic representation of the durability of the hydrophobic effectiveness of the coatings studied, based on the static water contact angles of the coated mock-ups prior to and after being subjected to the ageing process.

Figure 8 presents an assessment of the static water contact angles of samples after undergoing an ageing process, allowing us to evaluate the durability of the hydrophobic effectiveness of the coatings in comparison to their original conditions. Notably, sample L1 exhibits a substantial reduction in water contact angles, with FK-7 and CN2 coatings showing  $-2\%$  and  $-38\%$ , respectively. This indicates that these coatings experienced a decline in static water contact angles after ageing when compared to their untreated counterparts.

Figures 5–8 provide further insights into the durability of the hydrophobic effectiveness of the three coatings under evaluation. Coating FK-3 demonstrates notable resistance, given the minimal fluctuation in static water contact angles both before and after the ageing process. In contrast, coating FK-7 exhibits a positive degree of durability concerning hydrophobic effectiveness in aged marble samples and the non-carbonate reference sample G1 but less so in aged limestone and dolomite samples (Figures 5 and 7). Notably, standard deviation values are significant for samples M1 ( $94^\circ \pm 12$ ) and G1 ( $98^\circ \pm 7$ ), suggesting that this coating may not consistently meet the expected standards for hydrophobic effectiveness durability post-ageing.

Moreover, the static water contact angles of coating CN2 show a decrease following the ageing process (Figures 5 and 7). Considering the large standard deviation values of the static water contact angles in specimens coated with CN2, it is possible that this coating may, in most cases, offer acceptable durability in terms of hydrophobic effectiveness (Figures 7 and 8).



**Figure 8.** Enhancement (%) in hydrophobicity of studied stone samples for each applied coating after ageing compared with initial pre-treatment values.

These outcomes imply that the durability of hydrophobic effectiveness might be influenced by the chemical composition of the coatings employed. It is worth noting that while FK-3 and FK-7 are silane/siloxane-based, CN2 comprises modified silicon dioxide nanoparticles. Nevertheless, while the properties of the selected stone specimens, including their physical, chemical, and mineralogical attributes, cannot be overlooked, it was not possible to conclusively tie them to the coatings' hydrophobic durability.

### 3.4. Breathability Measurements

Coatings FK-7 and CN2 did not fulfil the required expectations in the chromatic change evaluation and mainly the assessment of the hydrophobic properties. As such, only samples coated with FK-3 were subjected to water vapour permeability measurements.

#### 3.4.1. Compatibility of Hydrophobic Coatings

Water vapour permeability test results for each stone sample before and after treatment and their difference in percentage are presented in Table 3.

**Table 3.** Water vapour permeability value of each stone sample before and after treatment, along with their difference (%).

Ref N.	Typology	Before Treatment	After Treatment	Difference
		( $\text{g m}^{-1} \text{s}^{-1} \text{Pa}^{-1}$ )	( $\text{g m}^{-1} \text{s}^{-1} \text{Pa}^{-1}$ )	%
L1	Limestone	$6.0 \times 10^{-12}$	$5.1 \times 10^{-12}$	-15
L2	Limestone	$6.3 \times 10^{-12}$	$5.9 \times 10^{-12}$	-6
L3	Limestone	$3.0 \times 10^{-12}$	$1.7 \times 10^{-12}$	-42
L4	Limestone	$8.9 \times 10^{-12}$	$4.6 \times 10^{-12}$	-49
L5	Calcitic dolomite	$7.7 \times 10^{-12}$	$4.0 \times 10^{-12}$	-48
M1	Marble	$2.2 \times 10^{-12}$	$1.2 \times 10^{-12}$	-46
M2	Marble	$4.7 \times 10^{-12}$	$3.9 \times 10^{-12}$	-17
M3	Marble	$5.1 \times 10^{-12}$	$3.7 \times 10^{-12}$	-29
M4	Marble	$3.8 \times 10^{-12}$	$2.2 \times 10^{-12}$	-42
G1	Granitoid	$5.5 \times 10^{-12}$	$3.5 \times 10^{-12}$	-36

Changes in water vapour permeability are one of the significant parameters for evaluating the harmlessness and compatibility of hydrophobic coatings after application [69].



This feature is of utmost importance because if, following the application of a coating, the permeability of water vapour significantly decreases, water may condense at the interface between the treated and untreated stone sections, creating mechanical stress that could initiate the decaying process [70]. In other words, a compatible hydrophobic coating should allow the surface of the stone to breathe.

According to Table 3, the water vapour permeability value of all the stone samples decreased after treatment, but the extent of this reduction varied among them. The specimens can, therefore, be subdivided into two groups: L1, L2, and M2 displayed lower reduction ranges (6–17%), while samples L3, L4, L5, M1, and M4 showed a higher percentage reduction (42–49%) in water vapour permeability after the application of FK-3.

Good compatibility with the stone substrate necessarily implies a low (or absence of) decrease in water vapour permeability, ensuring that the stone can “breathe”. It has been reported that the average percentage reduction in water vapour permeability for stones treated with hydrophobic coatings is 16.8% [28]. Therefore, samples L1 and L2 are considered within the acceptable range of water vapour permeability reduction (15% and 6%). However, it is important to note that the average percentage reduction reported by previous authors derived from a limited study and a larger dataset is necessary to establish a reliable acceptance threshold for water vapour permeability reduction of hydrophobic coatings.

Nevertheless, considering the value of 16.8%, samples L1 and L2 exhibited water vapour permeability reductions within acceptable ranges after coating application, emphasising their compatibility.

### 3.4.2. Hydrophobic Coatings Performance

Water vapour permeability test results for each stone sample before and after ageing and their difference in percentage are presented in Table 4.

**Table 4.** Water vapour permeability value of each stone sample after treatment and ageing process with their difference (%).

Ref N.	Typology	After Treatment	After Ageing	Difference
		( $\text{g m}^{-1} \text{s}^{-1} \text{Pa}^{-1}$ )	( $\text{g m}^{-1} \text{s}^{-1} \text{Pa}^{-1}$ )	%
L1	Limestone	$5.10 \times 10^{-12}$	$4.80 \times 10^{-12}$	−6
L2	Limestone	$5.93 \times 10^{-12}$	$5.15 \times 10^{-12}$	−13
L3	Limestone	$1.71 \times 10^{-12}$	$3.39 \times 10^{-12}$	98
L4	Limestone	$4.59 \times 10^{-12}$	$3.36 \times 10^{-12}$	−27
L5	Calcitic dolomite	$4.04 \times 10^{-12}$	$3.52 \times 10^{-12}$	−13
M1	Marble	$1.19 \times 10^{-12}$	$2.92 \times 10^{-12}$	145
M2	Marble	$3.90 \times 10^{-12}$	$3.04 \times 10^{-12}$	−22
M3	Marble	$3.65 \times 10^{-12}$	$3.61 \times 10^{-12}$	−1
M4	Marble	$2.16 \times 10^{-12}$	$3.35 \times 10^{-12}$	55
G1	Granitoid	$3.52 \times 10^{-12}$	$1.97 \times 10^{-12}$	−44

According to Table 4, water vapour permeability decreased in all the samples after ageing except in samples L3, M1, and M4. Moreover, the reduction for sample M3 is so low (~1%) that it can be considered as insignificant.

Weathering conditions can decrease the permeability of water vapour in normal situations, resulting in a reduction in the durability of the applied treatment [71]. However, the breathability of surfaces in corresponding samples can be influenced by positive values obtained during post and prior ageing [72]. Increased water vapour permeability can also be caused by the enhancement of open porosity in stones after artificial ageing [65]. Therefore, the increase in water vapour permeability in samples L3, M1, and M4 cannot be entirely related to the lack of durability of the applied coatings.

#### 4. Conclusions

In this study, three distinct coatings with different chemical compositions were selected: (i) FK-7 (composed of silane/siloxane derivatives), (ii) CN2 (modified silicon dioxide nanoparticles), and (iii) FK-3 (silane/siloxane and modified fluorinated additives). These coatings were compared by applying them to ten different stone specimens, including limestones, dolomite, marbles, and a granitoid, spanning a wide range and distinct genesis conditions. The physical, chemical, and mineralogical characteristics of all stone samples were determined to understand how these properties could correlate with the coatings' performance. Additionally, chromatic changes, hydrophobic properties, and breathability of treated and untreated stone samples were compared before and after coating application, as well as during the artificial ageing process, to shed light on their effectiveness, compatibility, and durability.

The results indicate that among the coatings tested, FK-3 demonstrated the greatest compatibility and enhancement of hydrophobic properties on the selected stones. Additionally, the FK-3 coating exhibited the greatest resistance to the artificial ageing method adopted for this study, indicating its potential for long-term protection in stone heritage. The superior performance of FK-3 can be attributed to its unique chemical composition, which includes modified fluorinated compounds alongside nano-silanes and siloxanes. While the correlation between effectiveness/durability results and the properties of the stones studied remains unclear, the presented data suggests a greater potential for improving the effectiveness of coatings when applied to low-porosity stones.

This contribution represents a significant step forward in the development of sustainable materials for stone protection and conservation. In this regard, the execution of this study has been of paramount significance in comprehending the behaviour and durability of coatings, particularly concerning their chemical composition. These research findings will contribute to advancing the design and production of novel coatings derived from natural and cost-effective compounds. This advancement is made possible by adjusting the composition, including the incorporation of fluorinated-based compounds, to enhance their functionality and durability. Furthermore, the incorporation of functionalised inorganic nanoparticles have the potential to significantly improve not only hydrophobic properties but also other essential characteristics. This opens new possibilities for the creation of highly effective smart-hybrid coatings. Therefore, the knowledge generated from this research provides a strong foundation for future advancements in the field of stone protection and conservation, enabling the creation of more sustainable, durable, and versatile coating solutions.

**Author Contributions:** Conceptualisation, L.D. and P.B.; methodology, F.A., L.D., V.P., F.S. and P.B.; validation, F.A., L.D., V.P., F.S., M.C. and P.B.; formal analysis, F.A., L.D. and M.C.; investigation, L.D. and P.B.; resources, J.M. and P.B.; data curation, F.A. and M.C.; writing—original draft preparation, F.A.; writing—review and editing, L.D., S.M., V.P., F.S., M.C. and P.B.; visualisation, F.A. and M.C.; supervision, L.D., J.M. and P.B.; project administration, P.B.; funding acquisition, J.M. and P.B. All authors have read and agreed to the published version of the manuscript.

**Funding:** This research was funded by Fundação para a Ciência e a Tecnologia (FCT) through the project Eco-STONEPROTEC—Eco-friendly superhydrophobic hybrid coatings for STONE PROTECTION (EXPL/CTA-GEO/0609/2021). The authors also acknowledge the financial support of the UIDB/04449/2020, UIDP/04449/2020 and LA/P/0132/2020 projects, funded by FCT and by the European Regional Development Fund. FA would also like to thank the Education, Audiovisual and Culture Executive Agency (EACEA) for her scholarship to attend the Erasmus Mundus Joint Master in ARCHAeological MATerials Science.

**Institutional Review Board Statement:** Not applicable.

**Informed Consent Statement:** Not applicable.

**Data Availability Statement:** The data presented in this study are available on request from the corresponding author.

**Acknowledgments:** The authors would like to thank to the anonymous companies that generously supplied commercial coating samples, enabling the execution of this study. Special acknowledgment is also extended to Fakolith for their collaboration and for providing their commercial products, which played a pivotal role in the research presented here.

**Conflicts of Interest:** The authors declare no conflict of interest.

## References

1. Price, C.A.; Doehne, E. *Stone Conservation: An Overview of Current Research*, 2nd ed.; Getty Publications—Getty Conservation Institute: Los Angeles, CA, USA, 2011; ISBN 978-1-60606-046-9.
2. Charola, A.E.; Price, C.A. Stone Conservation: An Overview of Current Research. *J. Am. Inst. Conserv.* **1998**, *37*, 223. [[CrossRef](#)]
3. Charola, A.E. Stone Deterioration Characterization For Its Conservation. *Geonomos* **2016**, *24*, 16–20. [[CrossRef](#)]
4. Lisci, C.; Pires, V.; Sitzia, F.; Mirão, J. Limestones Durability Study on Salt Crystallisation: An Integrated Approach. *Case Stud. Constr. Mater.* **2022**, *17*, e01572. [[CrossRef](#)]
5. Pires, V.; Amaral, P.M.; Simão, J.A.R.; Galhano, C. Experimental Procedure for Studying the Degradation and Alteration of Limestone Slabs Applied on Exterior Cladding. *Environ. Earth Sci.* **2022**, *81*, 59. [[CrossRef](#)]
6. Lisci, C.; Sitzia, F.; Pires, V.; Aniceto, M.; Mirão, J. Stone Endurance: A Comparative Analysis of Natural and Artificial Weathering on Stone Longevity. *Heritage* **2023**, *6*, 4593–4617. [[CrossRef](#)]
7. Morillas, H.; Maguregui, M.; Gallego-Cartagena, E.; Marcaida, I.; Carral, N.; Madariaga, J.M. The Influence of Marine Environment on the Conservation State of Built Heritage: An Overview Study. *Sci. Total Environ.* **2020**, *745*, 140899. [[CrossRef](#)] [[PubMed](#)]
8. Lee, C.H.; Lee, M.S.; Suh, M.; Choi, S.-W. Weathering and Deterioration of Rock Properties of the Dabotap Pagoda (World Cultural Heritage), Republic of Korea. *Environ. Geol.* **2005**, *47*, 547–557. [[CrossRef](#)]
9. Benavente, D.; de Jongh, M.; Cañaveras, J.C. Weathering Processes and Mechanisms Caused by Capillary Waters and Pigeon Droppings on Porous Limestones. *Minerals* **2020**, *11*, 18. [[CrossRef](#)]
10. Liu, X.; Koestler, R.J.; Warscheid, T.; Katayama, Y.; Gu, J.-D. Microbial Deterioration and Sustainable Conservation of Stone Monuments and Buildings. *Nat. Sustain.* **2020**, *3*, 991–1004. [[CrossRef](#)]
11. Ševčík, R.; Viani, A.; Machová, D.; Lanzafame, G.; Mancini, L.; Appavou, M.-S. Synthetic Calcium Carbonate Improves the Effectiveness of Treatments with Nanolime to Contrast Decay in Highly Porous Limestone. *Sci. Rep.* **2019**, *9*, 15278. [[CrossRef](#)]
12. Steiger, M.; Charola, A.E.; Sterflinger, K. *Stone in Architecture*; Siegesmund, S., Snethlage, R., Eds.; Springer: Berlin/Heidelberg, Germany, 2014; ISBN 978-3-642-45154-6.
13. Hosseini, M.; Karapanagiotis, I. *Advanced Materials for the Conservation of Stone*; Springer: Cham, Switzerland, 2018; ISBN 978-3-319-72259-7.
14. Barnoos, V.; Shekofteh, A.; Oudbashi, O. Experimental Evaluation of the Consolidation Treatments of Low Porosity Limestone from the Historic Monument of the Anahita Temple of Kangavar, Iran. *Archaeol. Anthropol. Sci.* **2022**, *14*, 63. [[CrossRef](#)]
15. Becerra, J.; Zaderenko, A.P.; Ortiz, R.; Karapanagiotis, I.; Ortiz, P. Comparison of the Performance of a Novel Nanolime Doped with ZnO Quantum Dots with Common Consolidants for Historical Carbonate Stone Buildings. *Appl. Clay Sci.* **2020**, *195*, 105732. [[CrossRef](#)]
16. Lakhani, R.; Sharma, R.K. *Strategies for the Restoration of Heritage Buildings: Material Issues*; CSIR-CBRI: New Delhi, India, 2018.
17. Karapanagiotis, I.; Manoudis, P.N. Superhydrophobic and Superamphiphobic Materials for the Conservation of Natural Stone: An Overview. *Constr. Build. Mater.* **2022**, *320*, 126175. [[CrossRef](#)]
18. Parkin, I.P.; Palgrave, R.G. Self-Cleaning Coatings. *J. Mater. Chem.* **2005**, *15*, 1689. [[CrossRef](#)]
19. Wang, Z.; Li, Y.; Jiang, L.; Qi, B.; Zhou, L. Relationship between Secondary Structure and Surface Hydrophobicity of Soybean Protein Isolate Subjected to Heat Treatment. *J. Chem.* **2014**, *2014*, 475389. [[CrossRef](#)]
20. Chindaprasirt, P.; Rattanasak, U. Fabrication of Self-Cleaning Fly Ash/Polytetrafluoroethylene Material for Cement Mortar Spray-Coating. *J. Clean. Prod.* **2020**, *264*, 121748. [[CrossRef](#)]
21. Liu, Q.; Zhang, B.-J. Syntheses of a Novel Nanomaterial for Conservation of Historic Stones Inspired by Nature. *Mater. Lett.* **2007**, *61*, 4976–4979. [[CrossRef](#)]
22. Melo, M.; Bracci, S.; Camaiti, M.; Chiantore, O.; Piacenti, F. Photodegradation of Acrylic Resins Used in the Conservation of Stone. *Polym. Degrad. Stab.* **1999**, *66*, 23–30. [[CrossRef](#)]
23. Wendler, E.; von Plehwe-Leisen, E. Water Repellent Treatment of Porous Materials. A New Edition of the WTA Leaflet. In *Proceedings of the 5th International Conference on Water Repellent Treatment of Building Materials*; Brussels, Belgium, 15–16 April 2008, Aedificatio Publishers: Freiburg, Germany, 2008; pp. 155–168.
24. Alvarez de Buergo Ballester, M.; Fort González, R. Basic Methodology for the Assessment and Selection of Water-Repellent Treatments Applied on Carbonatic Materials. *Prog. Org. Coat.* **2001**, *43*, 258–266. [[CrossRef](#)]
25. Munafò, P.; Goffredo, G.B.; Quagliarini, E. TiO<sub>2</sub>-Based Nanocoatings for Preserving Architectural Stone Surfaces: An Overview. *Constr. Build. Mater.* **2015**, *84*, 201–218. [[CrossRef](#)]
26. Artesani, A.; Di Turo, F.; Zucchelli, M.; Traviglia, A. Recent Advances in Protective Coatings for Cultural Heritage—An Overview. *Coatings* **2020**, *10*, 217. [[CrossRef](#)]
27. Ferrari, A.; Pini, M.; Neri, P.; Bondioli, F. Nano-TiO<sub>2</sub> Coatings for Limestone: Which Sustainability for Cultural Heritage? *Coatings* **2015**, *5*, 232–245. [[CrossRef](#)]

28. Aslanidou, D.; Karapanagiotis, I.; Lampakis, D. Waterborne Superhydrophobic and Superoleophobic Coatings for the Protection of Marble and Sandstone. *Materials* **2018**, *11*, 585. [[CrossRef](#)]
29. Zhang, Z.; Zhang, W.; Li, D.; Sun, Y.; Wang, Z.; Hou, C.; Chen, L.; Cao, Y.; Liu, Y. Mechanical and Anticorrosive Properties of Graphene/Epoxy Resin Composites Coating Prepared by in-Situ Method. *Int. J. Mol. Sci.* **2015**, *16*, 2239–2251. [[CrossRef](#)] [[PubMed](#)]
30. Frascá, M.H.B.O.; Yamamoto, J.K. Ageing Tests for Dimension Stone—Experimental Studies of Granitic Rocks from Brazil. In *Proceedings the 10th IAEG International Congress*; Nottingham, UK, 6–10 September 2006, The Geological Society of London: London, UK, 2006.
31. Zhao, J.; Gao, X.; Chen, S.; Lin, H.; Li, Z.; Lin, X. Hydrophobic or Superhydrophobic Modification of Cement-Based Materials: A Systematic Review. *Compos. Part B Eng.* **2022**, *243*, 110104. [[CrossRef](#)]
32. ISO 4287:1997; Geometrical Product Specifications (GPS) Surface Texture: Profile Method—Terms, Definitions and Surface Texture Parameters. ISO: Geneva, Switzerland, 1997.
33. Tang, H.; Cao, T.; Liang, X.; Wang, A.; Salley, S.O.; McAllister, J.; Ng, K.Y.S. Influence of Silicone Surface Roughness and Hydrophobicity on Adhesion and Colonization of Staphylococcus Epidermidis. *J. Biomed. Mater. Res. Part A* **2009**, *88A*, 454–463. [[CrossRef](#)] [[PubMed](#)]
34. Vázquez, P.; Luque, A.; Alonso, F.J.; Grossi, C.M. Surface Changes on Crystalline Stones Due to Salt Crystallisation. *Environ. Earth Sci.* **2013**, *69*, 1237–1248. [[CrossRef](#)]
35. Popov, Y.A.; Pribnow, D.F.C.; Sass, J.H.; Williams, C.F.; Burkhardt, H. Characterization of Rock Thermal Conductivity by High-Resolution Optical Scanning. *Geothermics* **1999**, *28*, 253–276. [[CrossRef](#)]
36. Zuena, M.; Ruggiero, L.; Della Ventura, G.; Bemporad, E.; Ricci, M.A.; Sodo, A. Effectiveness and Compatibility of Nanoparticle Based Multifunctional Coatings on Natural and Man-Made Stones. *Coatings* **2021**, *11*, 480. [[CrossRef](#)]
37. EN EN 1936; Natural Stone Test Method. Determination of Real Density and Apparent Density, and of Total and Open Porosity. British Standards Institution: London, UK, 2006.
38. Li, Y.; Dong, W.; Li, H.; Li, Z. Method of Vacuum Water Absorption to Determine the Porosity of Hardened Concrete. *Int. J. Struct. Civ. Eng. Res.* **2015**, *4*, 282–286. [[CrossRef](#)]
39. ASTM E96/E96M-14; Standard Test Methods for Water Vapor Transmission of Materials. ASTM International: Kansas City, MO, USA, 2014.
40. Andreotti, S.; Franzoni, E.; Degli Esposti, M.; Fabbri, P. Poly(Hydroxyalkanoate)s-Based Hydrophobic Coatings for the Protection of Stone in Cultural Heritage. *Materials* **2018**, *11*, 165. [[CrossRef](#)]
41. Sesana, E.; Gagnon, A.S.; Ciantelli, C.; Cassar, J.; Hughes, J.J. Climate Change Impacts on Cultural Heritage: A Literature Review. *WIREs Clim. Chang.* **2021**, *12*, e710. [[CrossRef](#)]
42. EN 15886:2010; Conservation of Cultural Property—Test Methods—Colour Measurement of Surfaces. European Standard: Brussels, Belgium, 2010.
43. Prieto, B.; Sanmartín, P.; Silva, B.; Martínez-Verdú, F. Measuring the Color of Granite Rocks: A Proposed Procedure. *Color Res. Appl.* **2010**, *35*, 368–375. [[CrossRef](#)]
44. Law, K.-Y. Definitions for Hydrophilicity, Hydrophobicity, and Superhydrophobicity: Getting the Basics Right. *J. Phys. Chem. Lett.* **2014**, *5*, 686–688. [[CrossRef](#)] [[PubMed](#)]
45. Wang, Z.; Elimelech, M.; Lin, S. Environmental Applications of Interfacial Materials with Special Wettability. *Environ. Sci. Technol.* **2016**, *50*, 2132–2150. [[CrossRef](#)] [[PubMed](#)]
46. Facio, D.S.; Mosquera, M.J. Simple Strategy for Producing Superhydrophobic Nanocomposite Coatings In Situ on a Building Substrate. *ACS Appl. Mater. Interfaces* **2013**, *5*, 7517–7526. [[CrossRef](#)] [[PubMed](#)]
47. De Ferri, L.; Lottici, P.P.; Lorenzi, A.; Montenero, A.; Salvioli-Mariani, E. Study of Silica Nanoparticles—Polysiloxane Hydrophobic Treatments for Stone-Based Monument Protection. *J. Cult. Herit.* **2011**, *12*, 356–363. [[CrossRef](#)]
48. Manoudis, P.N.; Karapanagiotis, I. Modification of the Wettability of Polymer Surfaces Using Nanoparticles. *Prog. Org. Coatings* **2014**, *77*, 331–338. [[CrossRef](#)]
49. EN 15802:2010; Conservation of Cultural Property—Test Methods—Determination of Static Contact Angle. European Standard: Brussels, Belgium, 2010.
50. Esposito Corcione, C.; De Simone, N.; Santarelli, M.L.; Frigione, M. Protective Properties and Durability Characteristics of Experimental and Commercial Organic Coatings for the Preservation of Porous Stone. *Prog. Org. Coatings* **2017**, *103*, 193–203. [[CrossRef](#)]
51. Yu, N.; Xiao, X.; Ye, Z.; Pan, G. Facile Preparation of Durable Superhydrophobic Coating with Self-Cleaning Property. *Surf. Coatings Technol.* **2018**, *347*, 199–208. [[CrossRef](#)]
52. ASTM G154C7; Resistance of a Nonmetallic Material to Simulated Sunlight and Moisture Exposure. ASTM International: West Conshohocken, PA, USA, 2006.
53. Lisci, C.; Sitzia, F.; Pires, V.; Mirão, J. Building Stones Durability by UVA Radiation, Moisture and Spray Accelerated Weathering. *J. Build. Pathol. Rehabil.* **2022**, *7*, 60. [[CrossRef](#)]
54. Tabor, D. Mohs's Hardness Scale—A Physical Interpretation. *Proc. Phys. Soc. Sect. B* **1954**, *67*, 249–257. [[CrossRef](#)]
55. Zeng, X.; Xiao, Y.; Ji, X.; Wang, G. Mineral Identification Based on Deep Learning That Combines Image and Mohs Hardness. *Minerals* **2021**, *11*, 506. [[CrossRef](#)]

56. Wahab, G.M.A.; Gouda, M.; Ibrahim, G. Study of Physical and Mechanical Properties for Some of Eastern Desert Dimension Marble and Granite Utilized in Building Decoration. *Ain Shams Eng. J.* **2019**, *10*, 907–915. [[CrossRef](#)]
57. Wang, Y.; Zhou, Q.; Li, K.; Zhong, Q.; Bui, Q.B. Preparation of Ni–W–SiO<sub>2</sub> Nanocomposite Coating and Evaluation of Its Hardness and Corrosion Resistance. *Ceram. Int.* **2015**, *41*, 79–84. [[CrossRef](#)]
58. Wenzel, R.N. Resistance of Solid Surfaces to Wetting by Water. *Ind. Eng. Chem.* **1936**, *28*, 988–994. [[CrossRef](#)]
59. Hu, Y.-Z.; Ma, T.-B. Tribology of Nanostructured Surfaces. In *Comprehensive Nanoscience and Technology*; Elsevier: Amsterdam, The Netherlands, 2011; pp. 383–418.
60. Amaral, P.; Correia, A.; Lopes, L.; Rebola, P.; Pinho, A.; Carrilho Lopes, J. On the Use of Thermal Properties for Characterizing Dimension Stones. *Key Eng. Mater.* **2013**, *548*, 231–238. [[CrossRef](#)]
61. Zhang, L. Aspects of Rock Permeability. *Front. Struct. Civ. Eng.* **2013**, *7*, 102–116. [[CrossRef](#)]
62. Costa, M.; Rousaki, A.; Lycke, S.; Saelens, D.; Tack, P.; Sánchez, A.; Tuñón, J.; Ceprián, B.; Amate, P.; Montejo, M.; et al. Comparison of the Performance of Two Handheld XRF Instruments in the Study of Roman Tesserae from Cástulo (Linares, Spain). *Eur. Phys. J. Plus* **2020**, *135*, 647. [[CrossRef](#)]
63. Gomes, E.M.C.; Fonseca, P.E. Eventos Metamórfico/Metassomáticos Tardi-Variscos Na Regiao de Alvito (Alentejo, Sul de Portugal). *Cad. Do Lab. Xeolóxico Laxe Rev. Xeol. Galega E Do Hercínico Penins.* **2006**, *31*, 67–86.
64. Mavromatis, V.; Goetschl, K.E.; Grengg, C.; Konrad, F.; Purgstaller, B.; Dietzel, M. Barium Partitioning in Calcite and Aragonite as a Function of Growth Rate. *Geochim. Cosmochim. Acta* **2018**, *237*, 65–78. [[CrossRef](#)]
65. Astilleros, J.M.; Pina, C.M.; Fernández-Díaz, L.; Putnis, A. The Effect of Barium on Calcite {104} Surfaces during Growth. *Geochim. Cosmochim. Acta* **2000**, *64*, 2965–2972. [[CrossRef](#)]
66. Malavasi, I.; Bernagozzi, I.; Antonini, C.; Marengo, M. Assessing Durability of Superhydrophobic Surfaces. *Surf. Innov.* **2015**, *3*, 49–60. [[CrossRef](#)]
67. Bayer, I.S. Superhydrophobic Coatings from Ecofriendly Materials and Processes: A Review. *Adv. Mater. Interfaces* **2020**, *7*. [[CrossRef](#)]
68. Chen, K.; Zhou, S.; Yang, S.; Wu, L. Fabrication of All-Water-Based Self-Repairing Superhydrophobic Coatings Based on UV-Responsive Microcapsules. *Adv. Funct. Mater.* **2015**, *25*, 1035–1041. [[CrossRef](#)]
69. Lettieri, M.; Masieri, M.; Aquaro, M.; Dilorenzo, D.; Frigione, M. Eco-Friendly Protective Coating to Extend the Life of Art-Works and Structures Made in Porous Stone Materials. *Coatings* **2021**, *11*, 1270. [[CrossRef](#)]
70. Scheerer, S.; Ortega-Morales, O.; Gaylarde, C. Chapter 5 Microbial Deterioration of Stone Monuments—An Updated Overview. In *Advances in Applied Microbiology*; Elsevier: Amsterdam, The Netherlands, 2009; pp. 97–139.
71. Roncon, R.; Borsoi, G.; Parracha, J.L.; Flores-Colen, I.; Veiga, R.; Nunes, L. Impact of Water-Repellent Products on the Moisture Transport Properties and Mould Susceptibility of External Thermal Insulation Composite Systems. *Coatings* **2021**, *11*, 554. [[CrossRef](#)]
72. Castelvetro, V.; Aglietto, M.; Ciardelli, F.; Chiantore, O.; Lazzari, M.; Toniolo, L. Structure Control, Coating Properties, and Durability of Fluorinated Acrylic-Based Polymers. *J. Coatings Technol.* **2002**, *74*, 57–66. [[CrossRef](#)]

**Disclaimer/Publisher’s Note:** The statements, opinions and data contained in all publications are solely those of the individual author(s) and contributor(s) and not of MDPI and/or the editor(s). MDPI and/or the editor(s) disclaim responsibility for any injury to people or property resulting from any ideas, methods, instructions or products referred to in the content.